Wave Load Prediction Methods in Offshore Wind Turbine Modelling and their Influence on Fatigue Load Analysis

Martin Kohlmeier[1], Kim Mittendorf[2], Thomas Kossel[1], Abderrahmane Habbar[1], Werner Zielke[1]

[1)] ForWind – Center for Wind Energy Research
Institute of Fluid Mechanics, Leibniz Universität Hannover, Germany
kohlmeier@hydromech.uni-hannover.de

[2)] Dr.techn.Olav Olsen Inc, Houston, Texas, USA
kem@olavolsen.com

Abstract:

The optimization of offshore wind turbines requires a design against extreme loads as well as fatigue loads. The latter is supposed to be more sensitive to a correct sea state modelling. Hence, wave load prediction methods with and without regarding the waves' directionality and spreading have been investigated with respect to their impact on damage equivalent fatigue loads. Simulation results have been compared with strain measurements at two different structures located in the North Sea. Finally, the consideration of the waves' directionality results in an approximate reduction of observed forces of up to 20% compared to the unidirectional approach.
Keywords: multi-component waves, directional spectrum, wave load modelling.

1 Introduction

Highly optimized and robust support structures for offshore wind energy converters are essential to make offshore wind energy economically promising. The design principles have to ensure a long life span and an extremely low failure rate.
Offshore wind energy farms are planned at locations of different water depths. They require appropriate types of support structures: monopile foundations are favoured in shallow and moderate water depths while in greater water depths tripod and jacket structures are considered to be advantageous.
Loads due to water waves represent a significant portion of the total environmental loads - especially in deep water - a profound understanding associated with a correct reproduction in numerical simulations are essential in order to gain satisfactory modeling results and a reliable design basis.
Waves entering shallow water show an increase in nonlinear behavior resulting in steeper crests and shallower troughs accompanied by a change in water particle kinematics. Usually, these waves are approaching the shore line in a more or less unidirectional way. In deeper water, however, the direction of the waves is varying according to the current sea state's origin.
In case of non-axis-symmetric support structures like jacket structures, the direction of a wave directly affects the response behavior. This could for example be demonstrated by analyzing the measured data at FINO 1 [13]. The resulting effects of a directional sea state description has been studied by Mittendorf [8] for the FINO 1 measurement platform.
In continuation of the above mentioned topic, the concern of this contribution is the further development of the modelling approach including the waves' directionality and the investigation of the influence of the spreading described by angular distribution functions. The resulting wave kinematics simulation and load prediction have been applied in analyses of the measurement mast "Amrumbank West". It results in an estimation of the influence of wave modelling strategies on fatigue quantities and finally on the life cycle assessment.
The chosen approach of sea state modelling is described in the ensuing section followed by a short review of wave load prediction and the estimation of damage equivalent loads used for fatigue analysis. Finally, in the fifth section the established modelling frame work is presented. It provides the interaction between elastodynamic analysis programs and several simulation tool like the developed wave kinematics and wave load module WaveLoads [14,8] as well as wind load modules. In the following section the applicability of this modelling approach is demonstrated within the context of investigation of the wind measurement mast "Amrumbank West".

2 Sea State Modelling

Commonly, sea states are described in terms of a wave spectrum, and the definition of an equivalent sea state in the time domain is possible from an inverse Fourier transform. In practice, it is necessary to use a discrete finite formulation, which can be interpreted as a superimposition of numerous linear waves (for velocity potential ϕ as well as for surface elevation η) with amplitudes and frequencies determined from the variance spectrum of water surface elevations and a random phase, see Borgman (1969) [1].
The velocity and acceleration field of the water particles can be derived directly from the potential ϕ. The contribution of the high frequency components to the velocity is exaggerated by an increased vertical displacement. Velocities reach a maximum near the surface under the crest, so the application of linear superposition in this region leads to an overestimation. Beneath the mean water level, this approach is in agreement with laboratory data (Dean and Perlin (1986) [2]) and shows a reasonable agreement. To compensate the model inadequacies near the surface, several stretching methods have been suggested in literature. For the following investigations a first order stretching formula by Wheeler [15] has been used. In the first order stretching techniques the effective water depth is modified using the instantaneous wave-free surface in computing the decay function.
In most cases real ocean waves still differ significantly from the preceding model assumption of irregular and long crested sea states. To get a more realistic simulation of sea state conditions, it is necessary not only to superimpose waves with different frequencies, amplitudes and phases, but also waves traveling in different directions (Fig.1).

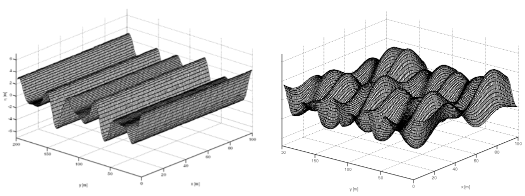

Figure 1: Unidirectional and directional irregular waves.

Forristall et al. [4] have observed considerable scatter between measured ocean wave velocities and the predictions of unidirectional theories with a clear bias toward over-prediction. Therefore the model of irregular ocean waves has been extended, so that the summation is made over frequencies and directions.

$$\phi(x,y,z,t) = \sum_i \sum_j a_{ij} \cdot \frac{g}{\omega_i} \cdot \frac{\cosh(k_i \cdot (h+z))}{\cosh(k_i \cdot h)} \cdot \sin\left(k_i \cdot \cos\theta_j \cdot x + k_i \cdot \sin\theta_j \cdot y - \omega_i \cdot t + \varepsilon_{ij}\right) \quad (1)$$

where
$a_{ij} = (2 \cdot S(f,\theta) \cdot \Delta\omega_i \Delta\theta_j)^{0.5}$: wave amplitude
$S(f,\theta)$: directional wave spectrum
ω: angular wave frequency
ε: random phase
k: wave number
h: water depth
g: gravity
t: time
x,y,z: spatial coordinates

The directional spectrum $S(f, \theta)$ represents the distribution of wave energy in the frequency domain and its directional spreading. It is given by the product of the variance spectrum $S(f)$ with a spreading function $D(f, \theta)$. The directional function of the 2D-spectrum has influence on the wave crest length and with it on the structure of the sea surface. Variation of the spreading function enables to simulate different sea state conditions like wind waves or swell as depicted in Fig. 2-4. In the following simulations, the $\cos^{2s}$-model by Mitsuyasu et al. [9]

$$D(\theta,\omega) = \frac{\Gamma(s+1)}{\pi^{0.5}\Gamma(s+0.5)} \cos^{2s}(\theta-\theta_0) \quad (2)$$

has been applied, where s is the spreading parameter.

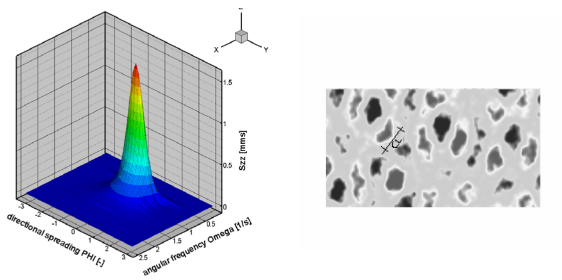

Figure 2: Directional JONSWAP spectrum (left) and a realization of the corresponding water surface elevation (right) for wind waves (H_s = 7.0 m, T_p = 11.0 s, spreading parameter s = 10).

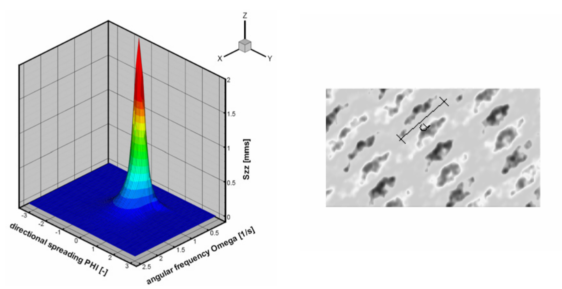

Figure 3: Directional JONSWAP spectrum (left) and a realization of the corresponding water surface elevation (right) for swell waves (H_s = 7.0 m, T_p = 11.0 s, spreading parameter s = 25).

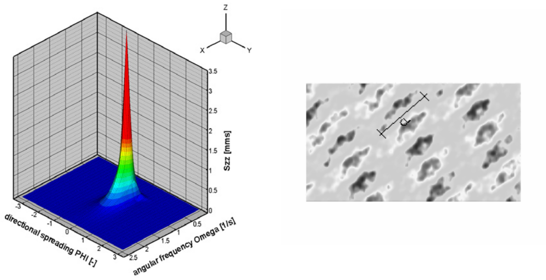

Figure 4: Directional JONSWAP spectrum (left) and a realization of the corresponding water surface elevation (right) for swell waves (H_s = 7.0 m, T_p = 11.0 s, spreading parameter s = 75).

3 Prediction of Wave Loading on Cylindrical Structures

We assume that the diameter D of the considered structure is small compared to the wave length L ($D/L < 0.2$). Then the structure appears to be transparent with respect to the waves' kinematics and consequently the diffraction and reflection effects of the waves can be neglected. Thus, the Morison equation [10] can be used to estimate the wave forces, composed by the inertia and drag force f_m and f_d, respectively, as follows

$$f \, \mathrm{d}z = f_\mathrm{m} + f_\mathrm{d} = c_m \rho \; \mathrm{d}V \frac{\partial u}{\partial t} + c_\mathrm{d} \frac{\rho}{2} \mathrm{d}A \, u \, |u| \, , \quad (3)$$

where c_m is the inertia coefficient, c_d is the drag coefficient, ρ the fluid density, $\mathrm{d}V = \mathrm{d}x \, \mathrm{d}y \, \mathrm{d}z$ is the differential volume, $\mathrm{d}A = \mathrm{d}x \, \mathrm{d}z$ is the differential cross section area and u is the fluid particle velocity orthogonal to the cylinder axis.

4 Estimation of Damage Equivalent Loads

The fatigue strength of the material is represented by the S-N curves (Wöhler curves). The S-N curve gives the number of cycles N which a specimen can resist before breaking versus the stress range ΔS. Usually the S-N curves are based on fatigue tests in the laboratory. Failure occurs, when a crack grows through the thickness of the component. Tests performed for different stress levels indicate: the lower the stress range the larger the number of bearable cycles. This can be described by a simple double logarithmic equation:

$$N_{failure}(\Delta S) = \frac{\Delta S_1^m}{\Delta S^m} = \frac{K}{S^m} \quad (4)$$

where
ΔS: stress range
ΔS_1: fictive stress range, gives failure after one single cycle
N_failure: number of cycles to structure failure
m: slope of curve, material dependent
K: reference number of cycles

The stress ranges S are defined as a series of closed hysteresis loops in the stress cycles. For the investigation of the structural response with respect to the fatigue behavior we have restricted ourselves to an analysis of the stress and bending moment resultants within a modified rainflow counting introduced by Rychlik [12].
With this, it is possible to perform further investigation of the fatigue damage for example with the Palmgren-Miner rule, which is a linear damage accumulation hypothesis where the order of load events is not noticed.

$$D_\mathrm{total} = \sum \frac{n(\Delta S_K)}{N_\mathrm{failure}(\Delta S_K)} \quad (5)$$

where
ΔS_k: k^{th} stress range
$n(\Delta S_k)$: actual number of cycles with stress range ΔS_k
$N_\mathrm{failure}(\Delta S_k)$: number of cycles to failure defined by S-N curve
D_total: accumulated damage

Consequently, the estimation of the total damage during the structures life cycle is beyond the scope of this work. In fact, the goal has been to evaluate the effect of different random wave models on the fatigue damage.
The study has been limited to selected sets of stationary sea states. The effect of different wave models has been compared in form of damage equivalent quantities (bending moments and/or stress ranges). A damage equivalent stress would lead to the same total damage for a given number of stress ranges n_E as the real observed stress collective. If the S-N curve is known, the damage equivalent stress range ΔS_E (normal force ΔN_E or moment ΔM_E) (see Fig. 5) can be calculated as follows

$$\Delta S_E = \left(\frac{1}{n_\mathrm{E}} \cdot \sum \left(\Delta S_i^m \cdot n_i \right) \right)^{1/m} . \quad (6)$$

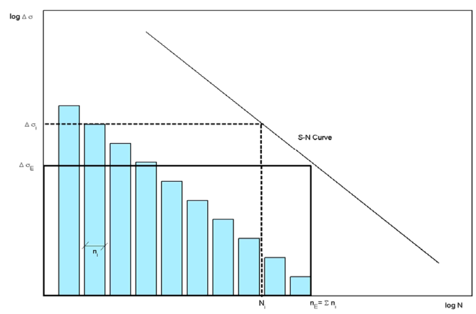

Figure 5: Damage equivalent stress range $\Delta\sigma_E$.

4 Simulation Framework for Integrated Modelling of OWECs

Three major aspects of integrated modeling have been set up in the current integrated modeling approach depicted in Fig. 6. The first aspect is concerned with the elasto-dynamic analysis that has been performed using the finite element program ANSYS coupled to environmental load module WaveLoads, see Mittendorf et al. [7] for details. Corresponding simulations can also be performed with the finite element program MSC.Nastran. Thus, modal analysis can easily be performed (Fig. 9).
The second aspect is concerned with multi-body dynamics including wave loading as well as wind loading and rotor blade dynamics in order to predict time series of stress resultants. This approach also gives the opportunity to investigate the interaction of the wind field and the rotor blade dynamics as well as the incorporation of different support structures using a modal description of its flexible compounds. With the modal description of the support structure provided by MSC.Nastran the multibody model can easily be extended towards different kinds of support structures ensuring fast and reliable simulations.

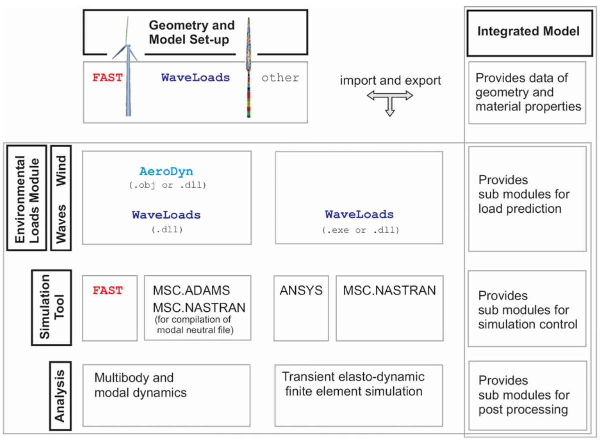

Figure 6: Finite element approach for elastodynamic analysis coupled to environmental loading.

The third aspect is concerned with the interaction and data interchange of software tools as the model set-up requires the interaction of the programs MSC.Adams, Fast [3], AeroDyn [6] and WaveLoads. All of these programs, which have different programming languages (Fortran 90 / C++), had to be combined as depicted in Fig. 7. In order to provide the required interfaces a dynamic link library (DLL) of the wave loading module WaveLoads has been developed and applied in graphical user interfaces as well as in the integrated simulation tools. This simulation framework provides a linkage of the wave load and the wind load modules and provides the interaction to different finite element analysis tools. Using this basis, the extension towards new requirements can be performed without great effort.

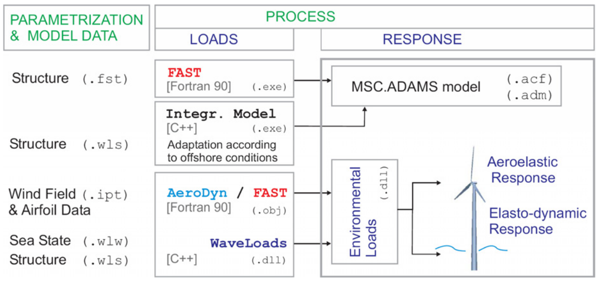

Figure 7: Data and program interaction in a multibody simulation approach.

5 Application of the Approach on a Monopile Support Structure

5.1 Set-up of the Finite Element Model of the Measurement Mast "Amrumbank West"

The wind measurement mast "Amrumbank West" is located approximately 36 km south-west of the island of Amrum in the North Sea (N 54°30', E 7°42'). The water depth is 22 m. The mast is a monopile construction rammed 23 m into the ground. It consists of the pile, a measurement chamber and a lattice mast up to a total height of 90 m above the mean water level.
The structure has been modeled with beam elements. Additional massless elements have been used to stiffen the structure for example in order to approximate the behavior of the measurement chamber. Accordingly, the weight of the transition piece and the measurement chamber has been condensed in mass points. The hydrodynamic mass is taken into account by increasing the density in the material properties of the beam elements between water surface and ground level. The foundation is modeled as elastic bedding with horizontal and vertical springs. The stiffness of the springs is determined using the bedding modulus method taking into account the skin friction and the point bearing pressure. More details can be found in Kossel [5].
In order to validate the structure model of the measuring mast "Amrumbank West" the results of a modal analysis were compared with results of the modal identification performed by Haake et al. [11] analyzing measured accelerations of the

structure. The evaluated mode shapes of the structure are depicted in Fig. 9. In an optimization process the concentrated mass points for the measurement chamber and the magnitude of hydrodynamic mass could be adjusted. The eigenfrequencies identified from the measurements are in good agreement with the corresponding eigenfrequencies predicted by numerical finite element analysis.

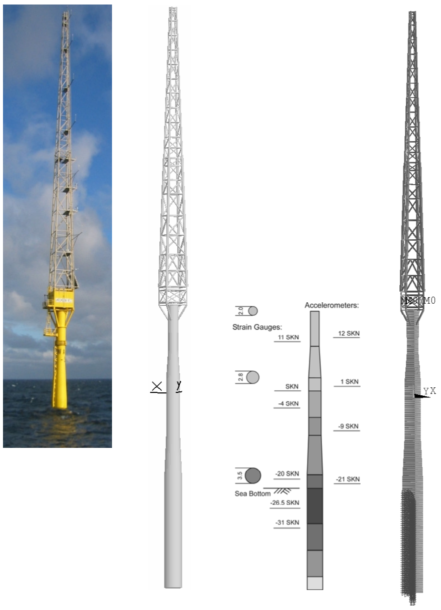

Figure 8: Photo of the measurement mast “Amrumbank West” and visualization of the structure used in WaveLoads (left). Depths of the location of strain and acceleration gauges installed at the support structure (middle) and the finite element model discretized by beam elements in the simulation program ANSYS (right).

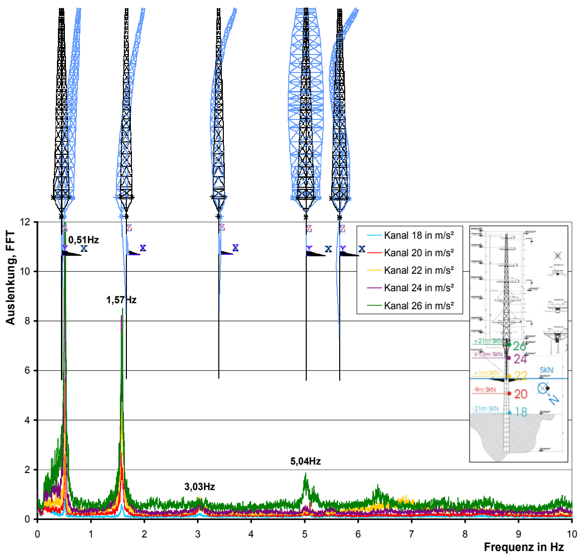

Figure 9: Validation of the finite element model by means of modal identification.

5.2 Application of Different Sea State Realizations

The water surface elevations at initial time $t_0 = 0$ s for different spreading parameter s is depicted in Fig. 10. For all realizations of sea states the same stochastic description has been used in order to get an impression of the resulting reduction in directional bandwidth with increasing spreading parameter s.

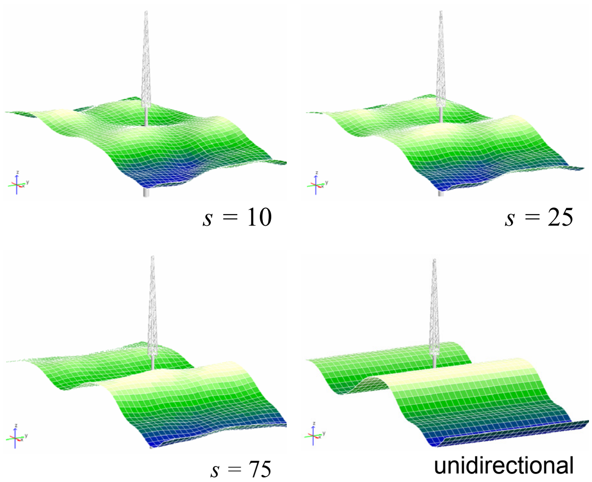

Figure 10: Water surface elevation (scaling factor: 5) of directional sea states with different spreading based on a directional JONSWAP spectrum ($H_s = 6.3$ m, $T_p = 12.5$ s).

In order to investigate the influence of the parameter s, four sets of 40 elastodynamic finite element simulations of 10 minutes length of the measurement mast loaded by random sea states of same significant wave height and peak period ($H_s = 6.3$ m, $T_p = 12.5$ s) but varying spreading parameter s=10, 25, 75 and 150 have been performed. According to the location of strain gauge measurements, the resulting damage equivalent loads due to bending moments in and normal to mean wave direction have been analyzed. The predicted results at the position of the strain gauge close to the mud line (Fig, 8) at a depth of SKN -26.5 m are depicted in Fig. 11 and 12.

The results show the dependency of the mean values of damage equivalent loads on the magnitude of the waves’ spreading. In comparison to the standard approach of simulating a unidirectional random sea state, the consideration of considerable spreading results in a reduction of damage equivalent loads if the mean wave direction is considered and increase if the direction normal to the mean waves direction is considered. In this special case of a monopole structure it can clearly be observed that the existence of directional wave spreading leads to local fatigue loads of significantly lower magnitudes.

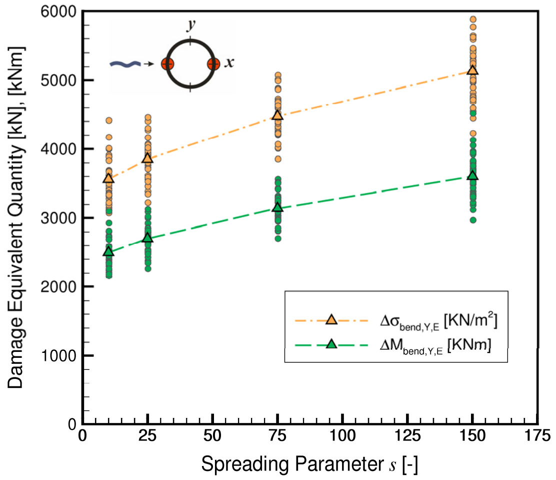

Figure 11: Resulting damage equivalent quantities vs. directional wave spreading parameterized by $s = 10, 25, 75$ and 150. The evaluation is based on stresses and bending moments caused by loads along the mean wave direction.

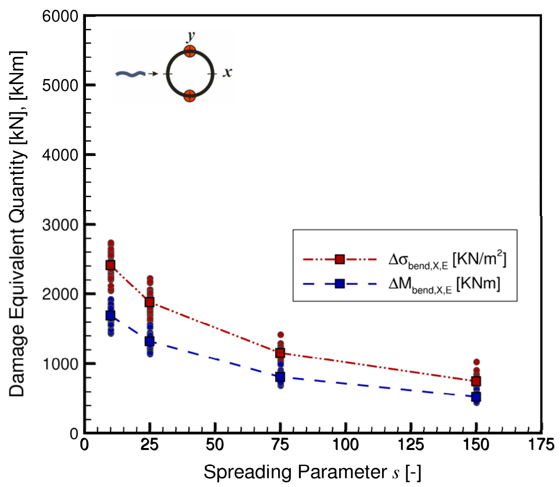

Figure 12: Resulting damage equivalent quantities vs. directional wave spreading parameterized by $s = 10, 25, 75$ and 150. The evaluation is based on stresses and bending moments caused by loads along the mean wave direction.

6 Conclusion

An integrated modelling approach for the investigation of the behaviour of support structures of offshore wind energy converters is being developed. Within an application on the support structure of the measurement mast "Amrumbank West" the influence of different wave models on damage equivalent fatigue loads has been investigated.

In-situ measurements have been used to validate the applied finite element model of the structure. According to the evaluated damage equivalent fatigue loads caused by wave loads from random wave simulation it can be concluded that the directional spreading described by an angular distribution function is a useful approach for modelling a more realistic sea state for the investigation of offshore structures in greater water depth.

A clear dependency of the mean values of damage equivalent loads and the magnitude of the waves' spreading could be observed. In comparison to the standard approach of simulating a unidirectional random sea state, the consideration of considerable spreading result in a reduction of damage equivalent loads of about 20 %. The investigation also demonstrated that due to the stochastic approach which is associated with significant variation in the resulting fatigue loads the number of simulations has to be increased significantly.

References

[1] Borgman, L. E., Ocean wave simulation for engineering design. *J. of the Waterways and Harbors Division*, 4:557 – 583, 1969.

[2] Dean, R. G. and Perlin, M., Intercomparison of near bottom kinematics by several wave theories and field and laboratory data. Coastal Engin., 9:399 – 437, 1986.

[3] Jonkman, J. M., Buhl Jr., M. L.: FAST User's Guide, NREL/EL-500-29798. Golden, Colorado: National Renewable Energy Laboratory, 2005.

[4] Forristall, G., Ward, E., Cardone, V. and Borgmann, L., The directional spectra and kinematics of surface gravity waves in tropical storm delia. *Journal of Physical Oceanography*, 83:888 – 909, 1978.

[5] Kossel, T., Wellenbelastungen auf die Tragstrukturen von Offshore-Konstruktionen. Diploma thesis, Institute of Fluid Mechanics and Computer Applications in Civil Engineering, Leibniz Universität Hannover, 2006.

[6] Laino, D. J., Hansen, A. C.: User's Guide to the Wind Turbine Aerodynamics Computer Software AeroDyn, 2002.

[7] Mittendorf, K., Kohlmeier, M., Habbar, A., Zielke, W.: Influence of irregular wave kinematics description on fatigue load

analysis of offshore wind energy structures. In: Proceedings of DEWEK 2006 – 8th German Wind Energy Conference, November 22-23, 2006, Bremen, Germany, 2006.

[8] Mittendorf, K.: Hydromechanical Design Parameters and Design Loads for Offshore Wind Energy Converters. Dissertation, Institut für Strömungsmechanik, Leibniz Universität Hannover, 2006.

[9] Mitsuyasu, H., Tasai, F., Suhara, T., Mizuno, S., Ohkusu, M., Honda, T., and Rikiishi, K. Observations of the directional spectrum of ocean waves using a cloverleaf buoy. *Journal of Physical Oceanography*, 5:750-760, 1975.

[10] Morison, J.R., O'Brien, M.P., Johnson, J.W. and Schaaf S.A., The Force exerted by Surface Waves on Piles, Pet. Trans., AIME, 189, pp. 149-154, 1950.

[11] Haake, G., Gerasch, W.-J., Rolfes, R. Validierte Strukturmodelle und System-identifikation. In: Zielke, W. (Editor) Annual Report GIGAWINDplus 2005, http://www.gigawind.de (in German).

[12] Rychlik, I., A new definition of the rainflow cycle counting method. *Int. J. Fatigue*, 9:119-121.

[13] Schaumann,P., Böker, C., Tragstruktur – Lebensdaueranalysen und Prognose-verfahren. In: Zielke, W. (Editor) Annual Report GIGAWINDplus 2005, http://www.gigawind.de (in German).

[14] Zielke, W., Mittendorf, K., Seegangs- und Wellenlasten. In: Zielke, W. (Editor) Annual Report GIGAWINDplus 2005, http://www.gigawind.de (in German).

[15] Wheeler, J., Method for calculating forces produced by irregular waves. Journal of Petroleum Technology, 359-367, 1970.